

ANALYSIS OF EQUI-INTENSITY CURVES AND  $N_{\mu}$  DISTRIBUTION OF EAS

G.TANAHASHI

Institute for Cosmic Ray Research, University of Tokyo  
Tanashi, Tokyo, 188 Japan

## ABSTRACT

The distribution of the number of muons in EAS and the equi-intensity curves of EAS are analyzed on the basis of Monte Carlo simulation of various cosmic ray composition and the interaction models. Problems in the two best combined models are discussed.

1. Introduction

Many analyses of EAS data have been reported to investigate the cosmic ray composition and their interaction. For example, the comprehensive work was reported by Gaisser et al(1) in 1978. After then, the equi-intensity data of Chacaltaya was revised(2) and the other data of Akeno experiment was added to it(3). Akeno experiment also gave a distribution of the number of muons( $>1\text{Gev}$ ) of EAS at fixed shower size with a good statistics(4). In this report we make an analysis of these data with use of the Monte Carlo simulation described in 2.

2. One dimensional simulation of EAS

Among the parameters used in the interaction model of the cosmic ray with the air nucleus, the collision m.f.p. is assumed to be  $\lambda = \lambda_0 / (1 + 0.07(\log E_0(\text{TeV}) + 1)^{1.5}) \text{gcm}^{-2}$  where  $\lambda_0 = 80$  and  $120$  for proton and pion interaction respectively, and  $E_0$  is the cosmic ray energy. The value of  $\lambda$  are shown in Fig.1 together with  $\sigma = 290.E_0(\text{TeV})^{0.06} \text{mb}$  obtained in the Akeno experiment(5). The assumptions of the other parameters are following.

The leading particle carries the energy  $E_s$  fluctuated uniformly between  $0-E_0$ . The partition of the rest of the energy between the fragmentation and the central region is half to half. The energy spectrum of the produced particles in the fragmentation is  $\exp(-E/E^*)$  where  $E^*$  is  $0.6E_s$  and  $E_s$  for proton and pion incident respectively. In the central region the spectrum is assumed to be a plateau shaped one whose energy spread is shown in Fig.2 for various models. Resultant multiplicity-energy relation, multiplicity distribution, scaling behavior and inclusive rapidity distribution are checked to fit the data of accelerator experiments. Produced particles are to be pions or kaons, and the proportion of the kaon production is to increase with the energy as  $0.05 \log E_0(\text{GeV})$ .

Interaction models shown in Fig.2 are used for the EAS calculation. They are SC(scaling), STD(standard, which is scaling + the extension of the central distribution in  $10^{14} \text{ev}$  to the higher energies), SC1/2(scaling + increasing multiplicity with  $E_0^{1/2}$  in the central region above  $10^{14} \text{ev}$ ), SCM(scaling + particles nearly at rest in CM system above  $10^{14} \text{ev}$ ) and CCM (no fragmentation particles and all particles nearly at rest in CM system above  $10^{14} \text{ev}$ ).

We have further two kinds, I and II, in each of the above models. I includes the generation of the high energy neutral pion as the leading particle, and the forward and backward symmetry of the produced particles in CM system. II includes no production of the energetic neutral pion as the leading, and the enhanced particle production in the backward three times more than the forward as the effect of target nucleus. The details

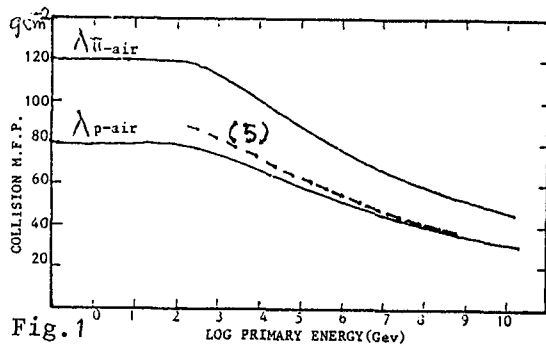


Fig. 1

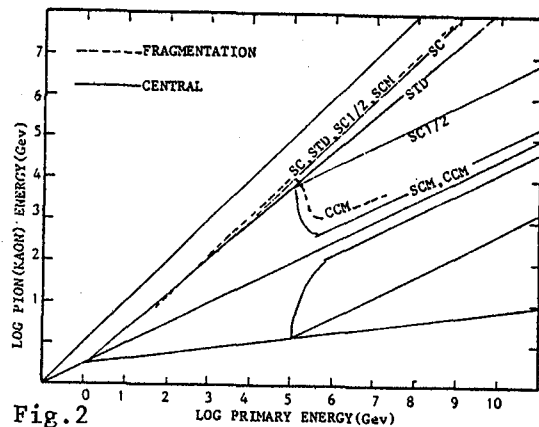


Fig. 2

of these assumptions will be described elsewhere.

The shower curves of electrons and muons of STD based on I, II are shown in Fig. 3. It is seen that the attenuation of particles between  $1000-1600 \text{ gcm}^{-2}$  is nearly exponential and has almost the same attenuation length ( $180-190 \text{ gcm}^{-2}$  in I and  $190-200 \text{ gcm}^{-2}$  in II) irrespective of the primary energies above  $10^{13} \text{ ev}$ . In the same figure, the shower curves of the constant cross section are also shown for the comparison. The reason that the attenuations are almost the same comes mainly from the increasing cross sections. The other result is that the muon content in II is almost 3 times larger than I's.

In Fig. 4 the shower curves of various models are shown in comparison. All of them are based on model I. It is found again the attenuation beyond  $1000 \text{ gcm}^{-2}$  are almost parallel. The difference among SC, STD and SC1/2 are very small, and this

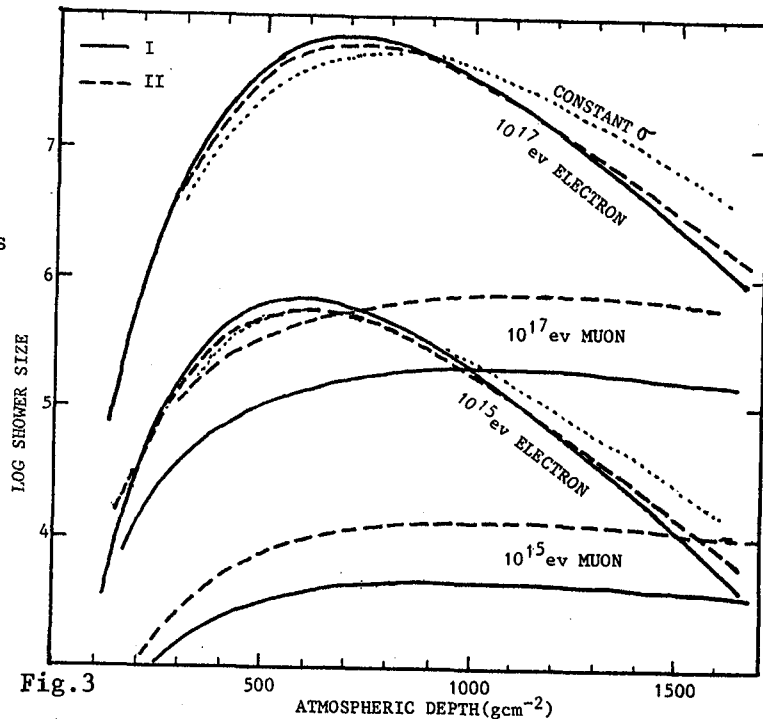


Fig. 3

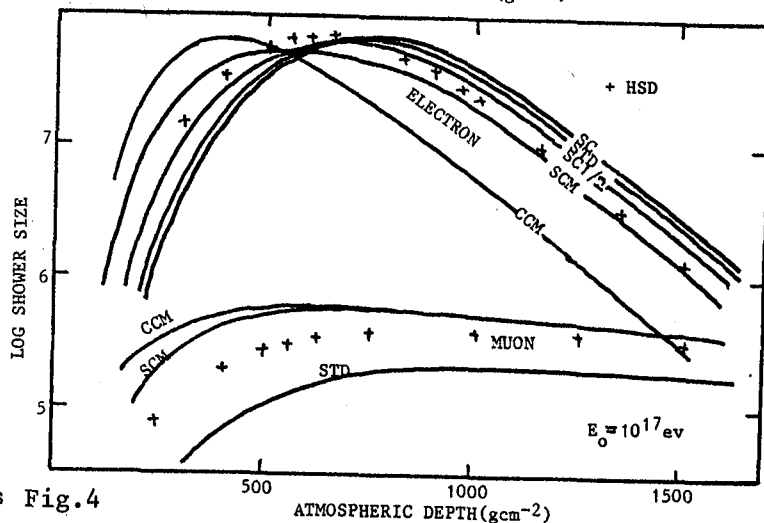


Fig. 4

means that the energy distribution in the central region does not affect much the shower curve except the extreme case like SCM. The crosses in the figure show the iron shower curve (HSD) based on the superposition of STD.

### 3. $N_{\mu}$ distribution of fixed $N_e$

The  $N_{\mu}$  distributions of EAS of different primary component (mass number  $A=1,4,15$  and  $50$ ) are calculated under the condition of fixed  $N_e$  assuming the primary integral energy spectrum to be  $E^{-2}$ . These  $N_{\mu}$  distributions include the error which comes into  $N_{\mu}$  in the course of the data reduction and also the error due to the possible fluctuation of muon lateral distribution. The distribution of  $A>4$  are almost due to these errors. These  $N_{\mu}$  distributions of each component are superposed to fit the experiment (5) as shown in Fig.5.

The conclusions obtained from this comparison are (i) low  $N_{\mu}$  tail requires the existence of proton showers more than

several % (ii) the  $N_{\mu}$  distribution of the proton shower must be as broad as in STD, that is, the very high multiplicity models are avoided because of their narrow distribution of  $N_{\mu}$  (iii) the average  $N_{\mu}$  of each component must be spread over more than

factor 3 for fixed  $N_e$ .

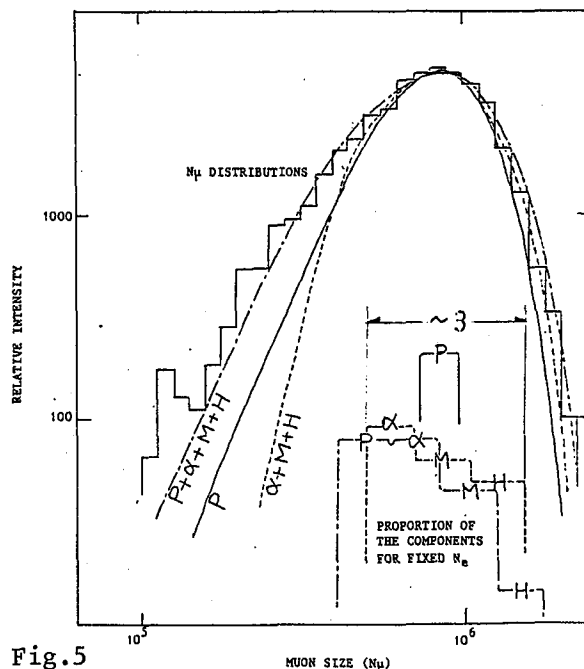


Fig.5

### 4. Equi-intensity curves of EAS

Equi-intensity curves of a mixed composition are related to each shower curves as follows. Assume that the shower curves are energy independent in the required energy region, that is  $N(E,x)=E \cdot N(x)$  where  $N(E,x)$  is the shower curve of energy  $E$  in depth of  $x$ . The intensity ratio of the heavy to the proton shower in fixed shower size is

$$\Delta(x) = (I_h/I_p)_{N_e} = (I_h/I_p)_E \cdot (N_h(x)/N_p(x))^{\gamma}$$

where  $k = (I_h/I_p)_E$  is the intensity ratio in fixed energy and  $\gamma$  is the integral exponent of the primary energy spectrum. Putting  $\gamma=2$ ,  $\Delta(x)$  can be calculated with use of the values of  $N_h(x)$ ,  $N_p(x)$  as the function of  $k$ . Equi-intensity curves  $\bar{N}(x)$  are obtained from

$$\bar{N}(x) = N_p(x) / (1 + \Delta(x)) + N_h(x) \cdot \Delta(x) / (1 + \Delta(x))$$

$\Delta(x)$  and  $\bar{N}(x)$  are calculated for the following combinations of the proton and the heavy showers.

proton shower	STD	STD	STD	SCM
heavy shower	HSD	SCM	CCM	CCM
notation	HSD/STD	SCM/STD	CCM/STD	CCM/SCM

The  $\bar{N}(x)$  are shown in Fig.6 for  $k=0.1, 1.0$  and  $10$  together with the experimental data (2) (3). In general, the attenuation length between  $800-1400 \text{ gcm}^{-2}$  are steeper than either prediction, but two cases (HSD/STD and  $k=10$ )

(CCM/SCM and  $k=0.1$ ) barely fit the experiment as shown in the figure in dotted curves after the normalization of the intensity. SCM/STD and CCM/STD do not fit because of too much difference of proton and heavy shower curves. This difference makes the composite curves flat.

### 5. Discussions and conclusion

Both two selected cases satisfy the requirement (i) in 3.

As for CCM/SCM, it is not clear whether (ii)(iii) are satisfied or not, but seems to be not. This model is introduced to approach the one which is proposed by Kakimoto et al(2) to explain the rapid development of EAS in high altitude observed by them. So the further progress of this experiment will test the model.

On the other hand, HSD/STD satisfies all the requirements (i)(ii)(iii) in 3. The problems of this model are the less content of muons in EAS and the slow development of the number of muons. The model needs about 2 times more muons. If we adopt model II instead of I, the number of muons increases but the attenuation length also increases apart further from the experiment. As for the slow development of muon in this model, we can scarcely fit the experiment by taking the number of muons of iron showers in  $600 \text{ g cm}^{-2}$  and of proton showers in  $1100 \text{ g cm}^{-2}$  (Fig.7). If the  $N_{\mu}$  difference of the proton and the heavy nucleus shower is larger in some model, such a model is better in this problem.

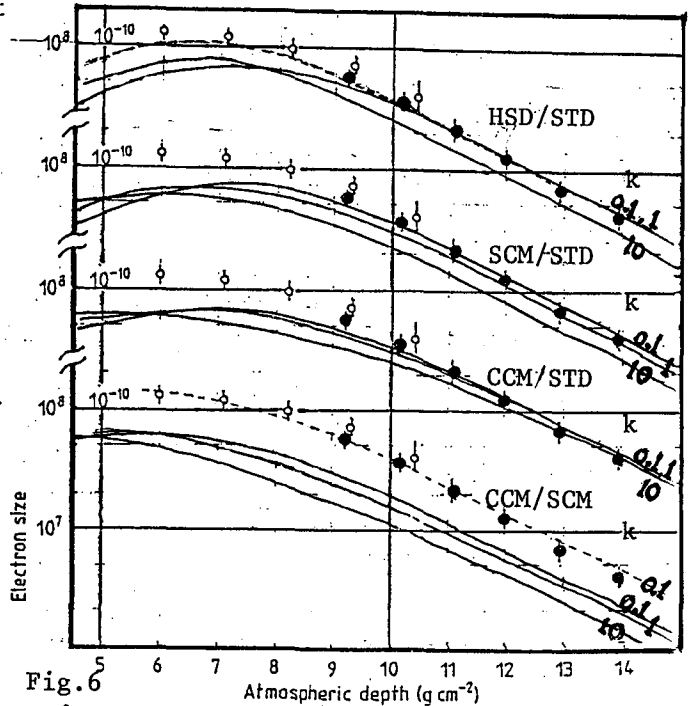


Fig.6

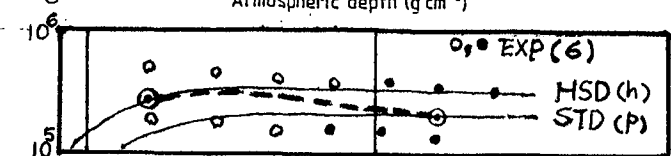


Fig.7

### Acknowledgements

The EAS simulation are done by FACOM 380 at the computer room, Institute for Nuclear Study, University of Tokyo.

### References

- (1) Gaisser, T.K. et al. Rev. Mod. Phys., 50, 859 1978
- (2) Kakimoto, F. et al. J. Phys. G; Nucl. Phys. 9, 339 1983
- (3) Nagano, M. et al. J. Phys. G; Nucl. Phys. 10, 1295 1984
- (4) Hara, T. et al. Proc. 18th ICRC(Banbalore), 11, 285 1983
- (5) Hara, T. et al. Phys. Rev. Lett. 50, 2058 1983
- (6) Hara, T. et al. Proc. 18th ICRC(Bangalore), 11, 281 1983